Biomed Microdevices (2017) 19:50
DOI 10.1007/s10544-017-0181-4

Nano-Calorimetry based point of care biosensor for metabolic disease management

Evan Kazura[1] · **Brad R. Lubbers**[1] · **Elliott Dawson**[2] · **John A. Phillips III**[3] · **Franz Baudenbacher**[1]

Abstract Point of care (POC) diagnostics represents one of the fastest growing health care technology segments. Developments in microfabrication have led to the development of highly-sensitive nanocalorimeters ideal for directly measuring heat generated in POC biosensors. Here we present a novel nano-calorimeter-based biosensor design with differential sensing to eliminate common mode noise and capillary microfluidic channels for sample delivery to the thermoelectric sensor. The calorimeter has a resolution of 1.4 ± 0.2 nJ/(Hz)$^{1/2}$ utilizing a 27 junction bismuth/titanium thermopile, with a total Seebeck coefficient of 2160 μV/K. Sample is wicked to the calorimeter through a capillary channel making it suitable for monitoring blood obtained through a finger prick (<1 μL sample required). We demonstrate device performance in a model assay using catalase, achieving a threshold for hydrogen peroxide quantification of 50 μM. The potential for our device as a POC blood test for metabolic diseases is shown through the quantification of phenylalanine (Phe) in serum, an unmet necessary service in the management of Phenylketonuria (PKU). Pegylated phenylalanine ammonia-lyase (PEG-PAL) was utilized to react with Phe, but reliable detection was limited to <5 mM due to low enzymatic activity. The POC biosensor concept can be multiplexed and adapted to a large number of metabolic diseases utilizing different immobilized enzymes.

✉ Franz Baudenbacher
franz.baudenbacher@vanderbilt.edu

[1] Department of Biomedical Engineering, Vanderbilt University, 5824 Stevenson Center, Nashville, TN 37235, USA

[2] BioVentures Inc., 1435 Kensington Square Court, Murfreesboro, TN 37130, USA

[3] Division of Medical Genetics and Genomic Medicine, Vanderbilt University School of Medicine, Nashville, TN 37235, USA

Keywords Calorimetry · Point of care · Biosensor · Thermopile · Phenylketonuria · Metabolic disease

1 Introduction

The expansion of point of care (POC) diagnostics over the past decade has allowed for near instantaneous results for many common blood tests that previously required expensive laboratory equipment and personnel time. With a worldwide market value of over $15.5 billion in 2013, POC diagnostics represents one of the fastest growing health care technology segments (Elder 2014). The largest POC segment, blood glucose monitoring, allows patients themselves to monitor blood glucose levels anywhere (Ben Mohammadi et al. 2015; Soni and Jha 2015). The information provided by the testing is essential for diabetic patients to regulate their glucose levels through medication and diet.

Biosensors are the basis for most POC diagnostic technologies. An enzymatic reaction with the analyte of interest produces a quantifiable signal transduced by one of several different methods; amperometric, optical, calorimetric, or acoustic to name a few (Danielsson 1982; De Corcuera and Cavalieri 2007). Calorimetry is an attractive detection method as most enzymatic reactions produce heat on the order of 20–100 kJ/mol substrate and are measured directly, not requiring the use of secondary or labeling reactions for transduction as most optical methods do (Danielsson 1990). Calorimetry is based on a temperature measurement and senses heat changes from chemical or physical processes present at the sensor, necessitating the elimination of noise from side reactions and temperature fluctuations (Lammers and Scheper 1999). Calorimetric biosensors of the past relied on flow-through columns with enzymes immobilized on a support matrix and thermistors for temperature sensing (Danielsson 1982). These required

Published online: 31 May 2017

large sample volumes (>0.5 ml), temperature controls, complex pumping systems, and were only suited to the laboratory setting (Lammers and Scheper 1997). Many were successful in measuring sub-milimolar concentrations of common blood analytes like cholesterol, urea, lactate, glucose, and ethanol (Lammers and Scheper 1999; Xie et al. 1999). The current trend is towards miniaturization, microfluidic sample handing, and on-chip thermoelectric based sensing (Verhaegen et al. 1999). In this way sample volume requirements are reduced to the microliter range and minimum detectable energies approaching 1 nJ are possible (Lee et al. 2009; Lubbers and Baudenbacher 2011). A few calorimetric biosensors suited to POC have been developed pertaining to the measurement of blood glucose or urine urea due to the large enthalpy changes associated with these reactions (−80 and −61 kJ/mol) (Davaji and Lee 2014; Lai and Tadigadapa 2012). In the case of Davaji and Lee, a thin film resistive temperature detector is employed, with a minimum detectable temperature change of 26 mK and noise limited minimum glucose concentration of 1.51 mM. A paper strip held the glucose oxidase enzyme in close proximity to the sensing surface, however enzyme was added to the flow strip at the beginning of each measurement, and evaporative effects caused a large drift in the calorimeter signal. Lai and Tadigadapa's device relied on a Y-cut quartz resonator for temperature sensing, giving higher temperature sensitivity. However, the entire device had to be placed in a 37 °C oven during measurements, microfluidic pumping systems were required, and the uncertainty in their urea detection results were too high for reliable use. In order to create a user-friendly calorimeter based POC device, common mode temperature signals must be eliminated, temperature sensitivity increased, sample volume reduced, liquid handing automated, and be insensitive to user error.

Phenylketonuria (PKU) represents another disease where at-home monitoring is needed to help effectively manage the disease. Affecting 1 in 15,000 people worldwide, PKU prevents the metabolism of the essential amino acid phenylalanine (Phe), leading to high blood concentrations that can cause mental retardation if not treated through diet and/or enzyme replacement therapy (Gamez et al. 2004). Though much faster and more accurate than the bacterial inhibition assays of the 1960's, tandem mass spectrometry (MS/MS) testing of blood Phe levels is still limited to larger scale clinical laboratories (Banta-Wright and Steiner 2004). At home Phe monitoring to dictate dosing and diet would save patients from constant visit to clinics and greatly improve their quality of life. With new enzyme replacement therapies for PKU undergoing human clinical trials, the need for Phe monitoring with immediate results to dictate dosing and diet is even greater. Towards the goal of POC Phe testing, we have developed a novel calorimetric biosensor with the ability to measure Phe levels in 1 μl of sample.

Here we present a novel nano-calorimeter-based biosensor design with differential sensing to eliminate common mode noise and capillary microfluidic channels for sample delivery to the thermoelectric sensor. Utilizing capillary forces for fluid movement is reliable and does not require external power or actuators (Chin et al. 2013). High sensitivity and ruggedness was achieved by the use of a suspended polymer membrane and bismuth/titanium thin film thermopiles. Catalase (CAT) and phenylalanine ammonia-lyase (PAL) are used in the detection of their respective substrates. Many common blood analytes (i.e. cholesterol, carbohydrates, and amino acids) have corresponding oxidases which release H_2O_2 during the oxidation of their substrate. The large enthalpy associated with H_2O_2 decomposition (−98 kJ/mol), can be exploited by co-immobilizing these enzymes with CAT, leading to enzymatic amplification of the signal (Lammers and Scheper 1999). Most oxidases require O_2 to react and this can be a limiting factor in closed systems since the O_2 saturation of water is only 0.25 mM. Alternative electron acceptors are used, but must be immobilized with the enzymes, increasing complexity and raising stability concerns. In the interest of reducing the number of immobilized components, we focused on systems not requiring external cofactors or enzyme cascades. PAL is one such enzyme, which catalyzes the conversion of l-phenylalanine to trans-cinnamic acid and ammonia with an enthalpy of +24.8 kJ/mol of Phe (Tewari et al. 1987). Here we present device design and characterization of the capillary calorimeter as well as preliminary data showing milimolar detection of Phe utilizing PAL with the potential of creating a robust at home test for the management of phenylketonuria.

2 Materials and methods

2.1 Reagents and materials

All micromachining was performed in the VIIBRE and VINSE cleanrooms at Vanderbilt University. 75 mm diameter silicon wafers, <100> orientation, double side polished, with 500 nm low stress silicon nitride (SiN) coated on both sides were obtained from WRS Materials (San Jose, CA). Chrome on soda-lime photomasks were fabricated by Front Range Photomask (Palmer Lake, CO). Photoresist and developer were purchased from MicroChem Corp. (Westborough, MA). PEG-PAL was donated by BioMarin (San Rafael, CA). Catalase (CAT) (#C100) and all other chemical are commercially available from Sigma-Aldrich (St. Louis, MO). All reactions were performed at room temperature.

2.2 Device modeling

Figure 1 shows the layout of the device including the differential sensing thermopile and capillary flow channel. As Fig. 1b shows, a low conductance suspended Su-8 membrane forms the top and bottom of the capillary channel around the

immobilized enzyme, reducing heat flux to the silicon substrate. The thickness of the capillary channel needed to be low enough to ensure fast wicking of the sample while minimizing the thermal conductance through the sample fluid itself.

A model of the calorimeter was built using COMSOL, and data output was analyzed in MATLAB. Unlike previous iterations (Lubbers and Baudenbacher 2011), the new design loses the radial symmetry of the freestanding drop calorimeter, which allowed for a simplified 2D model. Therefore, a full 3D model was constructed (Fig. 2a). In order to simplify the mesh construction of the thin freestanding membrane where the calorimeter sensing areas are located, the thermal properties of the thermopile metals and polymer membrane were combined and modeled together. A heat source representing the enzymatic reaction was placed as a cylinder within the sample liquid above the sensing junctions, and calorimeter sensitivity was determined by measuring the difference in temperature between the sensing and reference junctions. Temperatures at the two sensing areas were compared for 30 s, when both had returned to the baseline. The temperature difference was then integrated, converted to an expected voltage by multiplying by the total Seebeck coefficient of our thermopiles, then divided by the total energy produced by the heat source to return a sensitivity measurement in *V*/*W* (Fig. 3). Channel height, channel width, and sensing junction separation were varied individually and heat flow was modeled to maximize calorimeter sensitivity. Diffusion modeling within the sample liquid was employed to study the movement of substrate into the enzymatic reaction zone and determine if the reactions were diffusion or enzymatic rate limited.

2.3 Device fabrication

Fabrication of nanocalorimeters was performed using normal microfabrication techniques. Processing began by etching rectangular windows in the backside SiN layer by reactive ion etching, then anisotropically etching through the silicon in a potassium hydroxide bath, freeing SiN membranes on the frontside of the wafer. A uniform 0.5 μm thick Su-8 layer was deposited over the surface of the wafer, and hard baked until stable to serve as the base membrane for the nanocalorimeters. 200 nm of titanium was deposited by e-beam thermal deposition and patterned by a chemical wet etch of 30:1:1 parts water: hydrogen peroxide: hydrofluoric acid. We found an oxide layer formed on the titanium once exposed to the air, which greatly increased thermocouple resistance within the devices. A clean interface between the two metals of our thermopiles was integral in reducing thermopile resistance, and therefore the Johnson-Nyquist noise associated with it. This was accomplished by ion milling the surface of the titanium, then immediately depositing 400 nm of bismuth without breaking the chamber vacuum. E-beam thermal deposition was used to lay down the bismuth layer, and further ion milling was the method of patterning. In order to electrically insulate the thermopile circuits and protect the metal surfaces, a second 0.5 μm thick Su-8 layer was deposited as before on top of the devices. Reactive ion etching removed the remaining SiN from the backside of the Su-8, freeing the freestanding membranes and thermally isolating the nanocalorimeters from the wafer. An additional 50 μm thick Su-8 layer was patterned on the device surface to create interlocking spacers for the capillary channel (Fig. 1a). This ensured the top and bottom of the devices were always properly aligned. Device yield was good with less than 10% of devices rejected due to defective traces or broken membranes. Electrical contacts to the thermopile on the chip were built into a spring-loaded holder that also held down the sample lid during measurements. A custom-built low noise amplifier provided signal amplification (gain = 10,000) of the thermopile output voltage and data was recorded in LabVIEW. A 500 μm diameter, 50 nm thick gold spot was deposited through a shadow mask on each side of the thermopile to define a hydrophilic droplet wetting spot amid the hydrophobic Su-8 membrane.

2.4 Device characterization

The calorimeter time constant was measured by focusing a light beam onto one side of the differential thermopile and measuring the 1/e time to reach a steady state output voltage (Fig. 3a, b). This was measured while the device was filled with ~1 μl of distilled water. The actual volume of the capillary channel was ~275 nl, but the excess liquid ensured that the channel filled completely without bubbles and compensated for any evaporation of sample. Device sensitivity was measured using the enthalpy of dilution of Phe (+8.20 ± 0.05 kJ/mol at 298 K) (Kustov and Korolev 2007). Drops of 100 mM Phe in dH_2O at measured volumes between 5 and 20 nl were spotted onto one thermopile junction and evaporated. The calorimeter lid was reassembled and the device filled with dH_2O while measuring the thermopile output. Sensitivity was calculated by dividing the integral of the signal by the respective amount of Phe on the sensor. Phe has a negligible enthalpy change due to dilution below 100 mM, precluding the need to take into account the integral solution enthalpy. It also dissolves over a period of a few seconds, allowing the device to equilibrate after filling before the Phe has dissolved completely. The uncertainty in the sensitivity measurements (Table 1) are due to filling noise obscuring the first 500–1000 ms of the Phe dissolution (Fig. 3c).

2.5 Enzymatic measurements

The activity of CAT (EC 1.11.1.6) was measure by spectrographically monitoring the consumption of H_2O_2 at 240 nm in 50 mM phosphate buffered saline ph 7.4 (PBS). The activity

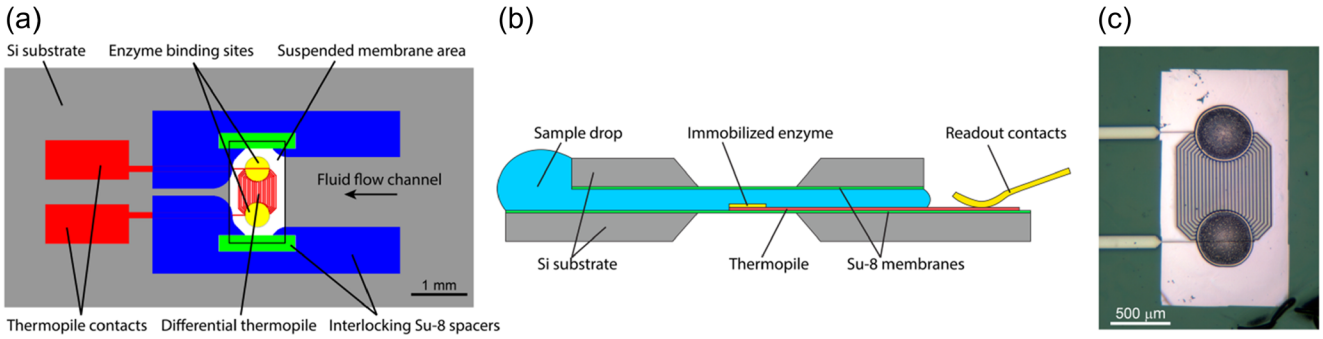

Fig. 1 Differential nanocalorimeter layout. **a** Active and control enzymes are bound to the two reaction zones read out by the 27 junction thermopile. The thermopile junctions are patterned on a suspended Su-8 membrane and line the edges of the enzyme spots to maximize sensitivity. The differential sensing arrangement eliminates errors associated with sample evaporation and heat of dilution. Interlocking Su-8 spaces on the top and bottom substrates allow for accurate alignment of the layers. **b** Device with immobilized enzymes on bottom substrate and capillary channel to deliver sample fluid. The suspended Su-8 membrane over the thermopile allows for very low thermal leakage, thereby maintain high sensitivity. When a sample drop (~1 µl) is placed at the device opening, capillary forces draw the sample into the reaction chamber in less than 1 s. (**c**) Image of the device with immobilized enzymes on the reaction zones

of PEG-PAL (EC 4.3.1.24) was measure by spectrographically monitoring the production of trans-cinnamic acid at 270 nm in 50 mM Tris-HCl pH 8.5 buffer. The reaction of CAT with hydrogen peroxide was used to demonstrate proof of concept of our differential calorimetric biosensor. CAT suspended in 50 mM phosphate buffered saline pH 7.4 (PBS) at 1000 units/ml was spotted onto the gold binding zone on one side of a sensor. PBS with 0.1 mg/ml bovine serum albumin (BSA) was spotted onto the other side of the differential sensor. Calibrated glass micropipettes were used to dispense 10 nl of solution for each spot. 1% PVA was added to the CAT/BSA suspension in most cases to aid in confining the enzyme after resuspension in the sample fluid. After assembling the lid onto the sensor and mounting in the device holder, 1 µl aliquots of PBS with H_2O_2 at concentrations between 0 and 2000 µmol were applied to an individual sensor channel. At higher concentrations of H_2O_2, O_2 generated by the reaction formed bubbles and resulted in inconsistent readings. After H_2O_2 application, the output signal was integrated over a period of 30 s and divided by the device sensitivity determined experimentally to obtain the total energy.

The quantification of Phe was accomplished using calorimetric detection with the enzyme PEG-PAL. Unmodified PAL has poor tolerance to desiccation, losing 50% activity upon exposure to moist air after drying (Rees and Jones 1996). Pegylated PAL was developed to decrease clearance rates when used for PKU therapy; however, the PEG group also increases tolerance to desiccation. We performed an activity assay utilizing PEG-PAL desiccated in the presence of 1% PVA and showed 86% activity retained. Due to the low activity of PAL (~ 2 units/mg), high concentration loading on the sensor surface is needed. PEG-PAL was supplied at 20 mg/ml in 150 mM NaCl, 10 mM tris-HCl pH 7.5. PVA was added to a final concentration of 1% *w/v* and 10 nl of the

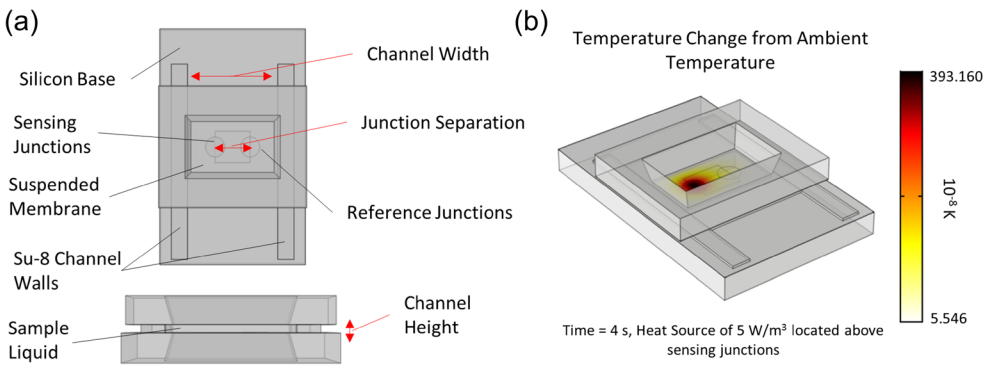

Fig. 2 3D model configuration for optimizing device sensitivity. **a** The COMSOL model consists of a 500 µm thick silicon base with a 1.5 µm thick Su-8 polymer layer on the top surface. A window in the base creates a free-standing membrane, on which are areas designated as the sensing junctions, reference junctions, and the thermopile tracks. Two Su-8 walls runs along the base, and a silicon lid with a matching thin membrane rest on top, forming a microfluidic channel. Parameters that were explored with regard to calorimeter sensitivity were the distance between the two channel walls (channel width), the height of the channel walls (channel height), and the distance between the sensing and reference junctions (junction separation). **b** Calorimeter sensitivity was predicted by running a heat transfer study and determining the temperature difference between the sensing junctions and reference junctions over time. A heat source of 5 W/m^3 was placed in a cylinder of radius 250 µm and height of 5 µm for 5 s to represent a reaction of the target analyte catalyzed by immobilized enzyme on the sensing area

enzyme mix spotted onto one enzyme binding spot on the differential calorimeter. Control enzyme was created by heating PEG-PAL suspension to 60 °C for 60 min before spotting 15 nl onto the control binding site. Assays showed no activity after heat treatment. Phe at 0–10 mM in 50 mM tris-HCl pH 8.3 was introduced into the assembled capillary calorimeter and monitored for up to 1 min. If more PEG-PAL was loaded onto the sensor surface, variance should decrease due to shorter integration times, so a second set of tests were run with PEG-PAL that was spin concentrated using Amicon Ultracel 30 K MWCO filters. However, the samples were too viscous to reliably pipette onto the sensor surface and dissolved inconsistently, leading to excessive errors.

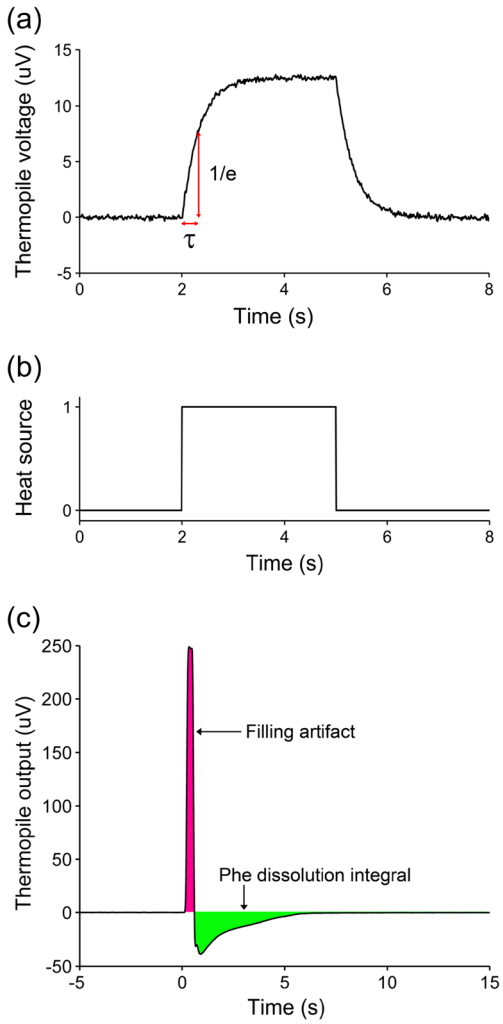

Fig. 3 Device characterization. **a** Device time constant was measured by pulsing a focused laser on the enzyme binding site while the device was filled with dH_2O. The time from pulse start to reciprocal of the natural exponent of the steady state voltage is the time constant. The typical τ for the filled device was 305 ± 5 ms (mean ± s.d., $n = 10$). **b** Laser pulse step function. **c** Sensitivity determination by Phe dissolution. The first 500–1000 ms of the signal is obscured until the device fills with water and the flow stops. The integral of Phe dissolution (green area) is used to calculate the power sensitivity of 7.2 ± 0.4 *V/W* (mean ± s.d., $n = 8$)

3 Results and discussion

3.1 Modeling design results

The results from the modeling guided the calorimeter design along the explored parameters. The configuration of the fluid sample was changed from a freestanding drop in previous calorimeter models to an enclosed channel. The membrane window was maximized with respect to stability to isolate the thermopiles from the high thermal conductance of the silicon wafer base. The calorimeter sensitivity was found to be inversely proportional with channel height (Fig. 4a). Similarly, a narrower channel also increased sensitivity of the device (Fig. 4b). As the volume of the liquid within the channel increased, so did its total heat capacity. This, combined with the higher thermal conductivity of the liquid relative to the Su-8 forming the membrane and walls of the channel (0.6 W/(m*K) and 0.2 W/(m*K), respectively), led to more heat being drawn away from the sensing elements embedded in the membrane, reducing sensitivity. These results guided the design process to balance reducing the channel cross section, in order to isolate the sample within from the wafer base, while still allowing for use without precise liquid measurement and placement. A height of 50 μm and width of 2355 μm were chosen as the smallest height and width while still allowing for easy sample loading by capillary forces.

The second major design change from previous iterations was moving the reference thermopile junctions of the calorimeter from over the silicon base to a differential mode onto the membrane within the sample channel. Previous designs had reference junctions radiating away from the thin membrane and located above the silicon wafer base, anchoring the reference temperature to room temperature with the comparably immense thermal conductivity of 149 W/(m*K). Calorimeter sensitivity was optimized by shortening thermopile length to reduce Johnson noise while ensuring the membrane was large enough to isolate the reaction (Lubbers and Baudenbacher 2011). The new design moves the reference junction to within in the microfluidic channel, allowing for a differential setup. By modeling a range of spacings between the sensing and reference junctions, calorimeter sensitivity was maximized

Table 1 Device properties. Means ± s.d. are shown ($n = 6$–18 per value)

Parameter	Symbol	Unit	Value
Thermal time constant	τ	ms	305 ± 5
Power sensitivity	P_{sens}	*V/W*	7.2 ± 0.4
Minimum detectable power	P_{min}	nJ/(Hz)$^{1/2}$	1.4 ± 0.2
Total thermal conductance	G_{tot}	μW/K	300 ± 24
Total Seebeck coefficient	S_{tot}	μV/K	2160
Effective thermal mass	C_{tot}	μJ/K	91.5
Thermopile resistance	R	kohms	11.5 ± 2.1

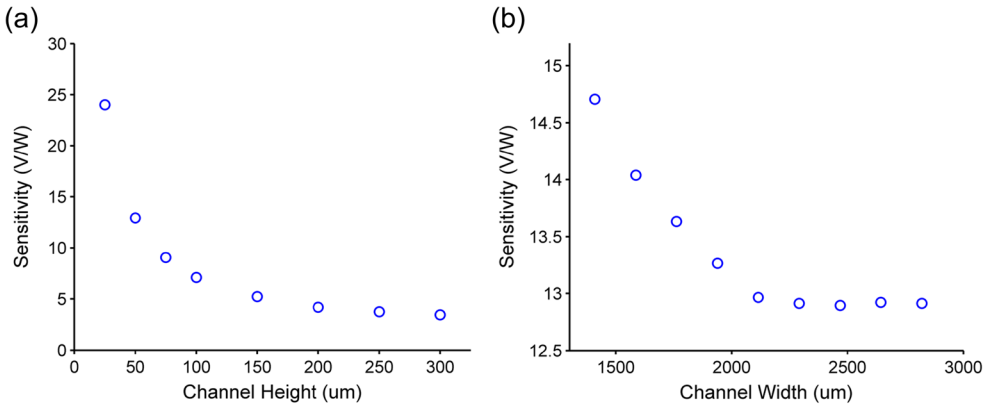

Fig. 4 Model Predictions of Sensitivity by Channel Dimensions. **a** The height of the channel walls was varied from 25 to 300 μm and resulting sensitivity was found. Decreasing the height reduces the total device heat capacity. 50 μm was chosen as the shortest height for the channel without complicating loading of the sample with clogging. **b** Holding the height at 50 μm, the spacing between the channel walls was simulated between 1410 and 2820 μm. Calorimeter sensitivity remained roughly constant until the walls were placed over the thin membrane, further isolating the liquid sample from the silicon base of the device

(Fig. 5). If the two areas were too close together, heat from the reaction zone above the sensing junction reached the reference junctions and decreased the overall temperature difference. If the junctions were close to the edge of the membrane, heat was lost at a greater rate through the silicon base. Combining this data with the increase in resistance from lengthening the metal thermopile tracks led to the optimal spacing of 910 μm. The model with this configuration of the microfluidic channel and thermopile calorimeter predicts a sensitivity of 12.9 *V/W.*

Peroxide diffusion modeling was then done to determine if a catalase-based reaction would be a proper assay to develop on our device. The time course of the reaction is largely determined by the diffusion of peroxide into the enzymatic reaction zone (Fig. 6). Diffusion modeling showed peroxide directly above the immobilized CAT is consumed in the first 3 s after sample addition. After local consumption, the reaction becomes diffusion limited, reducing the energy flux to a quasi-steady-state that persists for many second afterwards (Fig. 6b). Therefore, the energy integral is not significant affected by moderate changes in enzyme activity.

3.2 Device performance

As predicted by our COMSOL model, the addition of a fluid filled capillary channel reduced our device performance by a factor of 3 as compared to our previous nanocalorimeter in terms of power sensitivity, time constant, and minimum detectable power (Table 1). However, this still exceeds the minimum detectable energy of the next best microfluidic based calorimeter by a factor of 3 (i.e. 1.4 vs. 4.2 nW/Hz$^{1/2}$ for the Lee et al. device (2009)). Our device requires neither the vacuum insulation of the device by Lee et al., nor the use of pump and sacrificial channel fillers during fabrication. By utilizing a wide, 50 μm high channel, our device does not suffer from the clogging commonly associated with other microfluidic systems when flowing particle laded fluids like blood (Chin et al. 2013). The hydrophobic nature of the Su-8 making up the surface of the channel caused failures or incomplete filling, but was rectified by exposing the calorimeters to 30 s of oxygen plasma.

Since our device utilizes a closed configuration in conjunction with a differential sensing thermopile, evaporation effects are eliminated as shown by the steady baseline before and after filling (Fig. 3c). Originally, the filling noise created some error in the sensitivity determination, since the first 500–1000 ms of signal is lost and integration began after the final zero crossing. Signal variability was reduced by gating out the first 1000 ms of signal, regardless of the final zero crossing time.

3.3 Hydrogen peroxide assay

The differential sensing capillary calorimeter provides a new approach to POC testing of many blood analytes. We used the

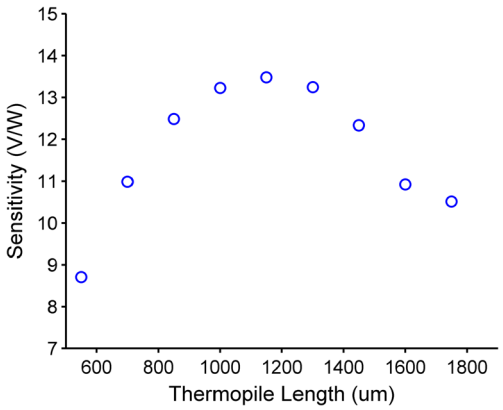

Fig. 5 Junction Separation Modeling. With the channel height and width held at 50 μm and 2355 μm, respectively, the effect of the distance between the sensing and reference junctions was simulated. A range of 550 μm to 1750 μm was explored. A maximum sensitivity of 13.5 *V/W* was found at 1200 μm between the junctions. However, the lengthening the thermopile tracks also increases Johnson noise from the resistance, so a junction separation of 910 μm was chosen

detection of H_2O_2 as a model system to demonstrate device performance and validate our model in terms of diffusion, enzyme kinetics and heat flow. Figure 7b shows that our measured data correspond well to the model predictions which could be used for correcting the signal during the filling of the device. This could aid in reducing error and extending our minimum detectable concentration. The energy integral correlates well with H_2O_2 concentration with a concentration uncertainty of ~75 μM below 500 μM (Fig. 7a). Measurements at 50 μM were significantly different from those at 0 mM ($P = 0.035$). When the amount of CAT bound to the sensor was reduced by one-half, the integral only decreased by 6% at the 1000 μM level.

Though currently not sensitive enough to measure normal H_2O_2 levels in the blood (~2.5 μm), H_2O_2 levels in urine levels are greater (up to 100 μM) and high levels are indicative of oxidative stress (Halliwell et al. 2000). Therefore our current device could be a useful tool for urinalysis and with further improvement could be applicable to blood peroxide determination. By measuring a signal integral over a finite time, rather than a rate as in most blood glucose POC sensors, our device is less sensitive to changes in enzyme activity. This is essential since CAT is not permanently immobilized to the sensor surface, buy rather dried onto it. If an excess of sample (i.e. > 1 μl) is added to the device, more enzyme is lost as it is swept away by the initial flow. Once flow ceases, the remaining enzyme stays localized due to the small diffusion coefficient of CAT

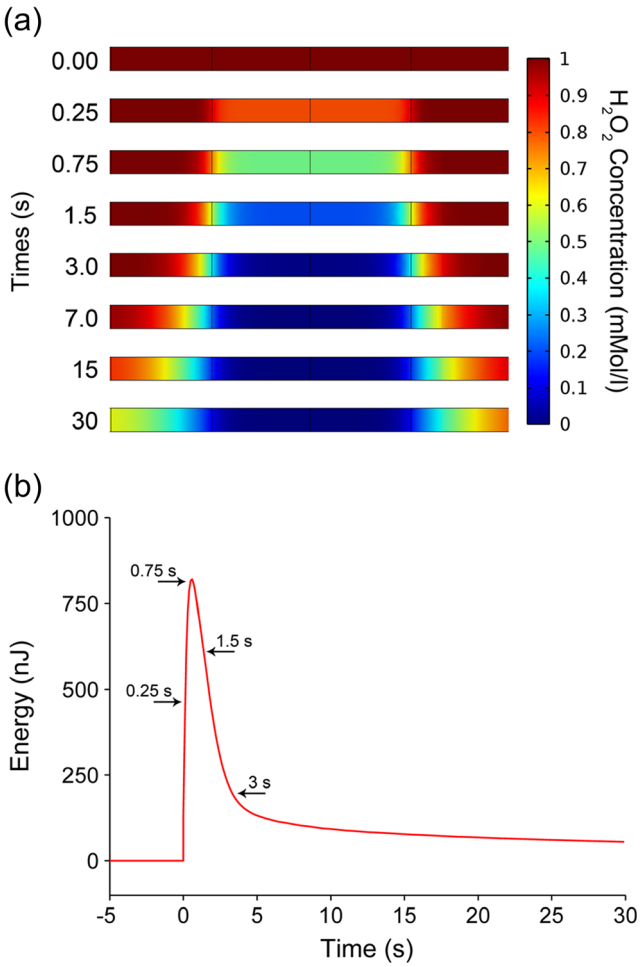

Fig. 6 Hydrogen peroxide diffusion modeling. **a** Side view of peroxide concentration from COMSOL modeling showed peroxide was quickly consumed by catalase at the local enzyme binding site. After 3 s peroxide consumption became diffusion-limited as the local concentration went to 0 mM. The left side is the dead end of the device, the right is the filling channel open to the reservoir. **b** The modeled thermal output from peroxide consumption shows a quasi-steady-state after local depletion. The steady state output is diffusion limited and the integrated signal is independent on the enzyme activity

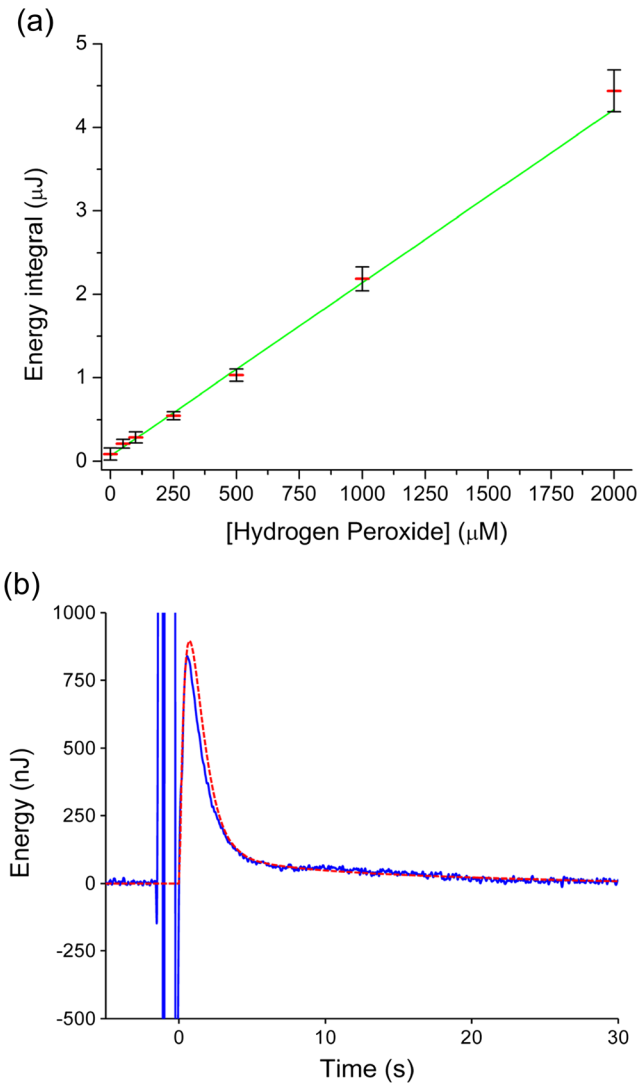

Fig. 7 Catalase assay. **a** Hydrogen peroxide concentration response when reacted with immobilized catalase on the capillary calorimeter. With a linear fit of $R^2 = 99.24$ and uncertainty of ±75 μM, a detection limit of 100 μm H_2O_2 can be achieved. Means ± s.d. are shown ($n = 4$ per point). **b** Representative output from 1000 μM H_2O_2 reacting with CAT overlaid with diffusion modeling results (red line). The instability of the signal before 0 s is due to the filling of the device and causes uncertainty in the energy integral since it partly obscure the signal

compared to H_2O_2 (4.1×10^{-7} vs. 1.3×10^{-5} cm^2/s) (Tyn and Gusek 1990). Other sources of error are related to the heat of dilution of the enzyme spots. If both spots are not of equal size and well centered on the thermopiles, unintended baseline shifts can occur. The gold spots currently used do not always limit the spread of liquid enzyme droplets before drying and devices with poorly matched spots were rejected. Future research, into techniques such as screen printing enzyme pastes are needed to improve sensitivity and robustness.

3.4 Phenylalanine assay

The calorimetric quantification of Phe by reaction with PEG-PAL showed that simple enzymatic reactions could be used to measure common blood analytes without the need for expensive optical or MS/MS systems. The energy integral correlated well with Phe concentration ($R^2 = 0.9295$), however noise at low concentrations limit the minimum detectable concentration to around 5 mM (Fig. 8b). As Fig. 8a shows, we can differentiate clearly between 5 and 10 mM but baseline drift prevents us from reliably detecting concentration of less than 5 mM. At 1 mM the detection was inconsistent compared to the CAT reactions with 1 mM H_2O_2 (i.e. ± 40% vs 6% error). Measurements at 1 mM were not significantly different from 0 mM readings ($P = 0.57$), but were at 5 mM and 10 mM ($P = 0.0039$) (Fig. 8b). Though this limit is well above the recommended Phe range for PKU patients (120–900 μM) (Longo et al. 2014), slight improvements would enable the device to be used for high level threshold detection. This would allow patients to detect abnormally high Phe levels at home, and report to their doctor for more thorough testing. We found that the pegylation of PAL helped preserve activity upon drying and helped to localize the enzyme to the thermopile upon rehydration with the sample fluid. As with the H_2O_2 assay, a main source of error was due to uneven dissolution of the enzyme spots, but was compounded by the lower reaction enthalpy and activity of PAL. With our diffusion model, we estimated 0.0078 units of CAT were present after sample addition, but only 0.0006 units of PEG-PAL remained. If another Phe reacting enzyme (i.e. phenylalanine 2-monooxygenase, EC 1.13.12.9) were used, which has potentially 50 times higher activity (Koyama 1982), sub-milimolar Phe detection would be possible. However, phenylalanine 2-monooxygenase does not have the commercial availability of PAL.

4 Conclusions

Compared to previous experiments performed on our standing drop nano-calorimeters (Lubbers and Baudenbacher 2011), error due to evaporation and heat of dilution upon sample injection is greatly reduced with our current design.

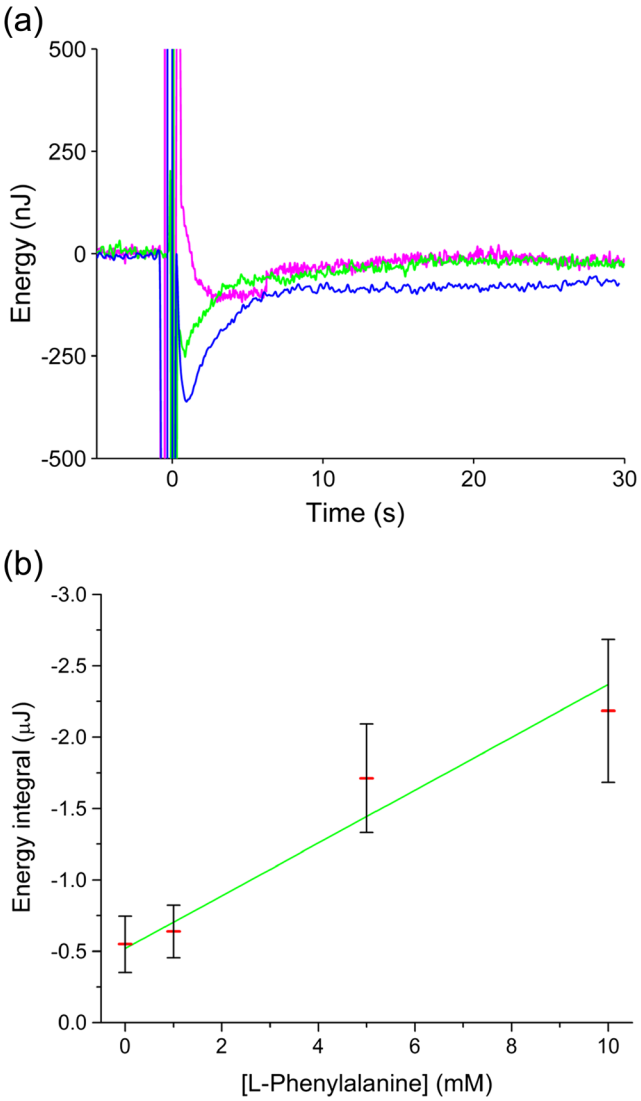

Fig. 8 Phenylalanine assay **a** Representative signals from 10 mM (blue), 5 mM (green), and 0 mM (magenta) Phe reacting on the capillary calorimeter. The low activity of PEG-PAL leads to a longer integration time and greater error associated with baseline drift. **b** Phe concentration response when reacted with immobilized PEG-PAL on the capillary calorimeter. Phe concentration confidence is lower with an $R^2 = 0.9295$ and uncertainty of ±3 mM. This is due to the lower activity of PEG-PAL compared to CAT, smaller reaction enthalpy, and greater error associated with rehydration of the dried PEG-PAL. Means ± s.d. are shown ($n = 4$ per point)

Utilizing a differential sensing approach eliminates theses errors and in combination with the capillary liquid handling eliminates the need for nanoliter scale sample handling making this approach ideally suited for a POC device. Even though sensitivity is reduced by a factor of 3, these devices still have the ability to measure milimolar concentrations of blood analytes. Since the space required for each thermopile is small (~1 mm^2), it would be possible to include several sensors in one capillary channel. These could provide control reactions, averaging to reduce noise, or monitor several analytes at once.

Acknowledgements This work was supported by a grant from BioVentures, Inc. We thank Raymond Mernaugh for assistance with enzyme binding and reactions.

References

S.A. Banta-Wright, R.D. Steiner, J. Perinat. Neonatal Nurs. **18**, 1 (2004)
L. Ben Mohammadi, T. Klotzbuecher, S. Sigloch, et al., Biomed. Microdevices **17**, 4 (2015)
C. Chin, S. Chin, T. Laksanasopin, S. Sia, In Point-of-care diagnostics on a Chip, ed. By D. Issadore, R.M. Westervelt (Springer, Berlin Heidelberg, 2013), p. 3
B. Danielsson, Appl. Biochem. Biotechnol. **7**, 1–2 (1982)
B. Danielsson, J. Biotechnol. **15**, 3 (1990)
B. Davaji, C.H. Lee, Biosens. Bioelectron. **59** (2014)
J.I.R. De Corcuera, R.P. Cavalieri, *Encyclopedia of agricultural, food, and biological engineering* (Taylor & Francis, 2007), pp. 119–123
M. Elder, Point of care diagnostics, BCC Res. Rep. (2014)
A. Gamez, L. Wang, M. Straub, M.G. Patch, R.C. Stevens, Mol. Ther. **9**, 1 (2004)
B. Halliwell, M.V. Clement, L.H. Long, FEBS Lett. **486**, 1 (2000)
H. Koyama, J. Biochem. **92**, 4 (1982)
A.V. Kustov, V.P. Korolev, Russ. J. Phys. Chem. A **81**, 2 (2007)
S.V.H. Lai, S. Tadigadapa, In Sensors, 2012 (IEEE, 2012), p. 1
F. Lammers, T. Scheper, Enzym. Microb. Technol. **20**, 6 (1997)
F. Lammers, T. Scheper, In Thermal biosensors, bioactivity, Bioaffinity, ed. By P.K. Bhatia, et al. (Springer, Berlin Heidelberg, 1999), p. 35
W. Lee, W. Fon, B.W. Axelrod, M.L. Roukes, Proc. Natl. Acad. Sci. U. S. A. **106**, 36 (2009)
N. Longo, C.O. Harding, B.K. Burton, D.K. Grange, J. Vockley, M. Wasserstein, G.M. Rice, A. Dorenbaum, J.K. Neuenburg, D.G. Musson, Z. Gu, S. Sile, Lancet **384**, 9937 (2014)
B. Lubbers, F. Baudenbacher, Anal. Chem. **83**, 20 (2011)
D.G. Rees, D.H. Jones, Enzym. Microb. Technol. **19**, 4 (1996)
A. Soni, S.K. Jha, Biosens. Bioelectron. **67** (2015)
Y.B. Tewari, E. Gajewski, R.N. Goldberg, J. Phys. Chem. **91**, 4 (1987)
M.T. Tyn, T.W. Gusek, Biotechnol. Bioeng. **35**, 4 (1990)
K. Verhaegen, J. Simaels, W.V. Driessche, et al., Biomed. Microdevices **2**, 2 (1999)
B. Xie, K. Ramanathan, B. Danielsson, In Thermal biosensors, bioactivity, Bioaffinity, ed. By P.K. Bhatia, et al. (Springer, Berlin Heidelberg, 1999), p. 1